Quantum Electronics **36** (10) 933 – 938 (2006)

CONTROL OF LASER RADIATION PARAMETERS

PACS numbers: 42.79.Ta; 42.60.Mi
DOI: 10.1070/QE2006v036n10ABEH013251

Use of neural-network systems to control transient multimode lasing

V.I. Ledenev

***Abstract*. A three-level neural network is considered which contains twenty five inputs, two hidden elements, and four outputs and is trained to recognise four situations at the input: the appearance of the fundamental mode of a Fabry – Perot resonator, the superposition of the fundamental and the first mode of the resonator with zero phases, the superposition of the fundamental and first mode of the resonator with phases 0 and π, and the appearance of the second mode and the superposition of the fundamental and second modes. It is shown that the network can recognise correctly variations in the mode composition of the Fabry – Perot resonator over the modulus of the transverse distribution of the field during the development of two-mode lasing. The operation of the network is studied for the two response times: the time shorter than the resonator time and the time determined by the response time of a pyroelectric detector of laser radiation.**

Keywords: *laser, Fabry-Perot resonator, lasing dynamics, numerical simulation, neural network*.

1. Introduction

The dynamics of transverse distributions of the laser emission field can be studied in detail by modern theoretical methods. Analytic investigations of the dynamics are based on the expansion of field and gain distributions in a set of orthogonal functions or in the modes of an empty resonator and description of the dynamics with the help of ordinary differential equations [1 – 4]. Such an approximation was used to study the bifurcation mechanisms of transitions between different lasing regimes and to analyse the rotation regimes of transverse distributions of the field and the formation of vortices [5 – 7]. An advantage of this approach is the possibility to solve ordinary differential equations by high-precision numerical methods allowing one to study the chaotic dynamics of the optical field. It was shown in [8] that the results obtained by this method in the case of stationary pumping coincide as a whole with numerical results obtained by the Fox – Lee method. However, the distribution profiles obtained by these two methods can have local differences within 10 % [8].

The numerical methods for determining the stationary types of oscillations in optical resonators are well developed at present [9 – 14]. The problem of finding these oscillations from the field distributions obtained upon successive round-trip transits of radiation in the resonator was formulated in [9], and algorithms of calculations by the methods of Prony, Krylov, and Arnoldi were presented in [9 – 14]. In particular, it was shown [12] for the complicated case of an unstable confocal resonator that the relative calculation accuracy of the eigenvalues and eigenvectors can achieve 10^{-11}. The preliminary determination of mode distributions specifies the initial conditions for calculating transient lasing in lasers with different resonators and constant pumping of the active medium [15, 16]. As a result, new types of lasing inherent in a laser as a distributed system were found [16] and the shape of modes and profiles of the gain in the nonlinear case were determined.

At present modes of higher orders than the fundamental mode are also used in technological laser processes. For example, radially polarised beams based on the first-mode field can be stronger absorbed in metal caverns than beams with different polarisations [17]. In this case, the admixture of the fundamental mode or higher-order modes in the light field is undesirable. On the other hand, in technological processes using the fundamental mode, the excitation of the first transverse mode is also undesirable because it gives rise to oscillations of the angular distribution of radiation. Therefore, the development of laser technologies requires the system to control the mode spectrum of lasers. The analytic and numerical methods developed at present can be used for the elaboration of such systems.

It is assumed in this paper that the near-field transverse radiation intensity distributions have specific features from which the number of generated modes and the relation between their amplitudes and phases can be found (such distributions are presented, for example, in [18]). Modern methods for controlling the mode composition do not require the determination of these features. It is sufficient to use neural networks (NNs) trained to recognise the required situations [19, 20]. The situations considered in this paper are the appearance at the NN input either of the fundamental mode of a Fabry – Perot resonator or the superposition of the fundamental and first modes of the resonator with zero phases, or the superposition of the fundamental and first modes with phases 0 and π, or of the second mode or the superposition of the fundamental and second modes.

V.I. Ledenev Institute on Laser and Information Technologies, Russian Academy of Sciences, Svyatozerskaya ul. 1, 140700 Shatura, Moscow region, Russia; e-mail: ledenev_ilit@rambler.ru

Received 22 May 2006
Kvantovaya Elektronika **36** (10) 933 – 938 (2006)
Translated by M.N. Sapozhnikov

2. The neutral network

Figure 1 shows a radiation source, the arrangement and design of a NN. It is assumed that the NN has a classical three-level structure with twenty-five input neurons, two neurons in the hidden layer, and four neurons in the output layer. The response of neurons is described by the sigmoid function [19]. It is assumed that photodetectors in the first layer are small compared to the distribution width and can be considered as point sources.

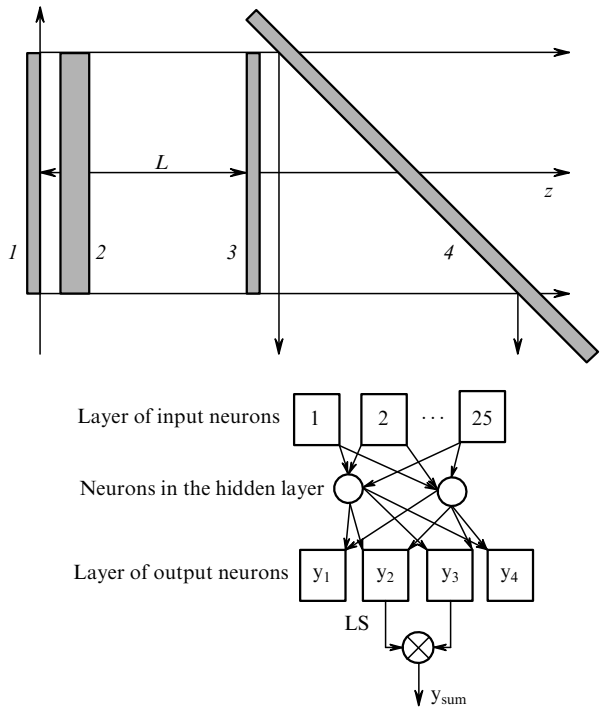

Figure 1. System for control of the mode composition of laser radiation: (*1*, *3*) Fabry–Perot resonator mirrors; (*2*) active-medium layer; (*4*) beamsplitter; (*L*) distance between mirrors; (LS) logical scheme giving the value $y_{sum} = y_2$ or $y_{sum} = y_3$ if y_2 or y_3 are greater than 0.5.

First the mode composition of an empty Fabry–Perot resonator was determined in the numerical experiment and a set of examples for NN training was created based on this composition. The set used here consisted of 33 distributions grouped according to the number of output neurons. The first group contained the $a(j)|U_0(x)|$ distributions. When distributions from this group entered the NN input, the first output neuron y_1 should give the value equal to unity and the other three neurons $y_2 - y_4$ should give zero. The second and third groups contained distributions $a(j)|U_0(x) + b(l)U_1(x)|$ and $a(j)|U_0(x) - b(l)U_1(x)|$, respectively. For these input distributions, the conditions $y_2 = 1$ (y_1, y_3, $y_4 = 0$) and $y_3 = 1$ (y_1, y_2, $y_4 = 0$) should be fulfilled. The fourth group contained distributions $a(j)|U_2(x)|$ and $a(j)|U_0(x) + b(l)U_2(x)|$. In this case, $y_4 = 1$ ($y_1 = y_2 = y_3 = 0$). In the expressions presented above, $U_{0,1,2}(x)$ are distributions of the complex amplitudes of the fundamental, first, and second modes, respectively; j, $l = 1, 2, 3$; $a_{1,2,3} = 0.8, 0.9, 1.0$; $b_{1,2,3} = 0.1, 0.2, 0.3$. Thus, the NN was trained by this set of examples to recognise at its input not specific distributions but some of their forms such as the fundamental mode, two superpositions of the fundamental and first modes, and superpositions including the second mode (the NN was not adjusted to recognise the mode amplitudes).

Two methods of training were used: the method of backward propagation and evolution approach [19, 20]. In the latter case, training was performed by changing generations. In each generation, a population was formed with individual species representing a set of the weights of hidden and output neurons randomly perturbed with small amplitude. The number of species in the population was ~ 100. The population was formed by using the elite strategy [20]: the most successful species from the previous generation passed to the next generation (i.e. the species recognising input distributions in the best way) and the rest of the members of the population were formed based on this species during mutations (random perturbations of weights). Thus, the next generation could not deteriorate the recognition of the mode forms. Species were not crossed despite recommendations [20]. Nevertheless, the training occurred rather rapidly. Figure 2a shows the time dependence of the root-mean-square error of the network output for the most successful species. One can see that the error decreased from ~ 1 to 10^{-90} for 6 min. During this time, 6000 generations have changed. One can see from Fig. 2b that the curve is not smooth, i.e. the evolution weakened sometimes. This occurred when no species improving the population were found in the corresponding generation.

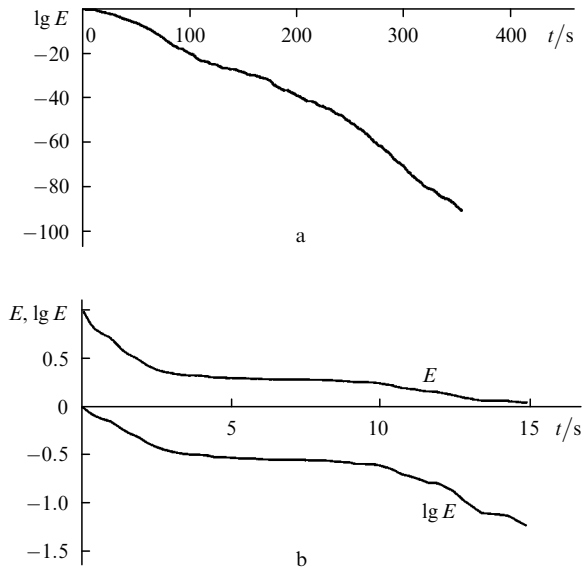

Figure 2. Time dependence of the logarithm of the root-mean-square error of the outputs of the NN on the training set (a) and slowing down of the training rate in the absence of proper species in the population (b).

According the NN structure, its hidden layer should in fact compress information on the input distribution to two bits. The least successful values of the outputs of neurons of the hidden layer for each of the four groups were $(1.17 \times 10^{-3};\ 9.95 \times 10^{-1})$, $(3.18 \times 10^{-10};\ 1.81 \times 10^{-4})$, $(1.00;\ 1.00)$ and $(9.97 \times 10^{-1};\ 2.46 \times 10^{-4})$, respectively. One can see that during the evolution the hidden layer was trained to number groups by bits (0; 1), (0; 0), (1; 1), (1; 0). Nevertheless, the error in the hidden layer is not such small as that in the output layer, i.e. the NN compensated

errors of the operation of the hidden layer in the output layer. Note that training by the method of backward propagation occurred much slower.

3. The calculation scheme

Transient lasing was calculated in a plane geometry. In the small-angle approximation of the scalar diffraction theory, the electric field E in the resonator was represented in the form of counterpropagating plane waves modulated by smooth envelopes F and B:

$$E(x,z,t) = [F(x,z,t)\exp(\mathrm{i}k_0 z) + B(x,z,t)\exp(-\mathrm{i}k_0 z)\exp(-\mathrm{i}\omega_0 t). \quad (1)$$

Here, ω_0 is the carrier frequency and $k_0 = \omega_0/c$. The dynamics of the envelopes $F(x,z,t)$ and $B(x,z,t)$ of the forward and backward waves, respectively, was described by the equations

$$2\mathrm{i}k_0\left(\frac{1}{c}\frac{\partial B}{\partial t} - \frac{\partial B}{\partial z}\right) + \frac{\partial^2 B}{\partial x^2} - \mathrm{i}k_0 g B = 0, \quad (2)$$

$$2\mathrm{i}k_0\left(\frac{1}{c}\frac{\partial F}{\partial t} + \frac{\partial F}{\partial z}\right) + \frac{\partial^2 F}{\partial x^2} - \mathrm{i}k_0 g F = 0. \quad (3)$$

The waves satisfy the reflection conditions at mirrors:

$$F(x,0,t) = -B(x,0,t)r_1, \quad (4)$$

$$B(x,L,t) = -F(x,L,t)r_2. \quad (5)$$

Here, r_1 and r_2 are the reflection coefficients of the highly reflecting and output mirrors, respectively, and L is the distances between the mirrors. The amplification of radiation in the active medium was described by the equation

$$\tau\frac{\partial g}{\partial t} = g_0(x) - g(1+I), \quad (6)$$

where $I = |F|^2 + |B|^2$ is the radiation intensity averaged over the interference oscillations of counterpropagating waves and normalised to the saturation value [21]. Thus, the calculations took into account simulated emission and relaxation with the time constant τ.

The initial condition $F(x,0,0)$ for the forward wave was specified with the help of the distribution of the fundamental mode $U_0(x)$. The initial condition $B(x,0,0)$ for the backward wave was found with the help of the round-trip transit of radiation in the resonator. The amplitudes of the initial distributions of the forward and backward waves and the initial distribution of the gain were chosen close to their stationary values. This made it possible to compare the calculations of single-mode lasing by expressions (2)–(6) with analytic results for weak perturbations [21].

The Fabry–Perot resonator had the following parameters: the radius of mirrors $a = 1$ cm, the distance between mirrors $L = 150$ cm, the reflection coefficients $r_1 = 1$ and $r_2 = 0.8$, the resonator Fresnel number $N_F = 6.25$. The threshold gain of the fundamental mode was $g_t = 1.5337 \times 10^{-3}$ cm^{-1}, the pump excess over the threshold was $k = g_0/g_t$, and the relaxation time was $\tau = 10^{-5}$ s. Thus, the physical parameters of the problem corresponded to those used in [15]. The differences were that the active medium was only one thin layer adjacent to the first mirror (in [15], the active-medium layer was located in the middle of the network element along the z axis) and the diffraction step was performed by calculating the Fresnel–Kirchhoff integral (in [15], the spectral approach was used). The size of the grid in the transverse direction was $M_x = 257$. Calculations were performed for the pump excess over the threshold $k = 1.34 - 1.55$. Distributions corresponding to small values of k proved to be the most difficult for recognition; for this reason, the time dependences are presented below for $k = 1.347$.

4. The fast-response neural network

The time dependence of the radiation power P_{out} on the output mirror in the interval 0–320 μs is shown in Fig. 3a. The region of the curve between 0 and 220 μs corresponds to single-mode lasing, and region AB corresponds to the generation of the fundamental mode of constant amplitude. Figure 3b presents the time dependences of the power P_{out} without the constant component for the point model (curve with a smaller amplitude) and calculation scheme (2)–(6). One can see that the curves are in good agreement although the calculation model is greatly simplified. The theoretical period T_d of relaxation oscillations found in the point model [21] was 5.96 μs. The numerical experiment gave the

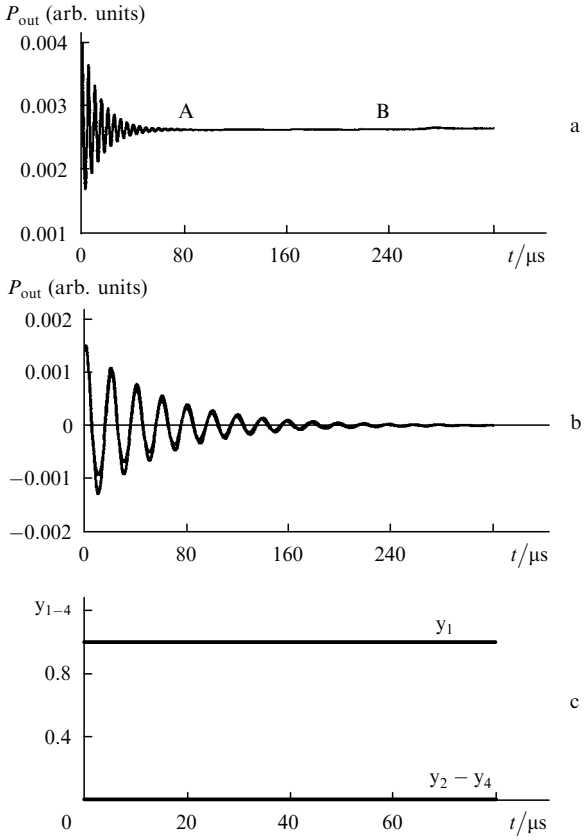

Figure 3. Time dependences of the radiation power P_{out} on the output mirror (A is the region of single-mode lasing; B is the region of a passage to two-mode lasing) (a) and of the power P_{out} without the constant component for the point model (curve with a smaller amplitude) and for the calculation scheme (2)–(6) (b), as well as the NN outputs in the region A (c).

value 5.91 μs with a root-mean-square deviation of 0.003 μs^{-1}. Similarly, the attenuation coefficient δ_d for the point model was 0.0675 μs^{-1}, while its calculated value was 0.0706 μs^{-1} for the root-mean-square deviation of 0.006 μs^{-1}. Such deviations correspond as a whole to results [15]. Therefore, the calculation scheme is valid for studying transient lasing regimes.

Figire 3c shows the output signals $y_1 - y_4$ of the NN in region A in the case of a fast response of the network (the response time is smaller than the round-trip transit time for radiation in the resonator). One can see that $y_1 = 1$, while other output signals y_2, y_3, and y_4 of the NN are equal to zero. Thus, the NN correctly recognised the single-mode lasing regime.

Upon passing to two-mode lasing ($t > 200$ μs), the average emission power P_{out} on the output mirror increases weakly ($\sim 0.5\,\%$) and is unnoticeable in Fig. 3a. Figure 4a presents the envelope of the oscillation amplitude of the angular maximum of the far-field radiation (to demonstrate oscillations themselves, the time scale should be much smaller). Figures 4b–c show the NN outputs $y_1 - y_3$ for a fast response (for each round trip in the resonator). The output $y_4 = 0$ is not shown in Fig. 4. One can see the NN correctly recognised the change in the lasing regime in the region of 240 μs. The intermediate region, in which the value of y_1 was between 0 and 1, had a width of ~ 40 μs (Fig. 4b). After the end of the intermediate region, the value of y_1 was stabilised at zero – the NN ceased to observe single-mode lasing, and the values of y_2 and y_3 (Figs 4c, d) showed the appearance of the first mode. However, y_2 and y_3 also take zero and intermediate values. The reason is explained in Fig. 5, which shows the positions of the angular maximum φ_{max} of far-field radiation at small time intervals (Fig. 5a) and neuron outputs y_2 and y_3, which, as follows from Figs 5b, c, correspond to the variable deviations of the angular radiation maximum from the resonator axis. The use of the logical scheme (see Fig. 1) considerable improves the recognition (Fig. 5d). The value $y_{sum} = 0$ corresponds to the phase shift between the fundamental and first modes equal to $\pm\pi/2$.

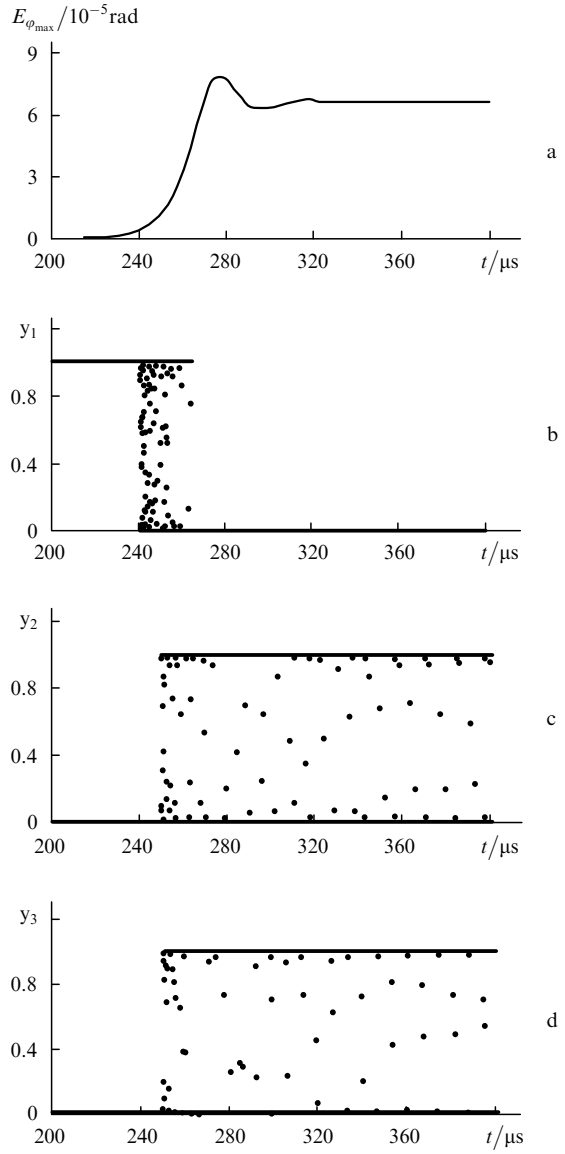

Figure 4. Time dependence of the envelope of the shift of the central far-field radiation maximum (a) and the NN outputs $y_1 - y_3$ (b–d).

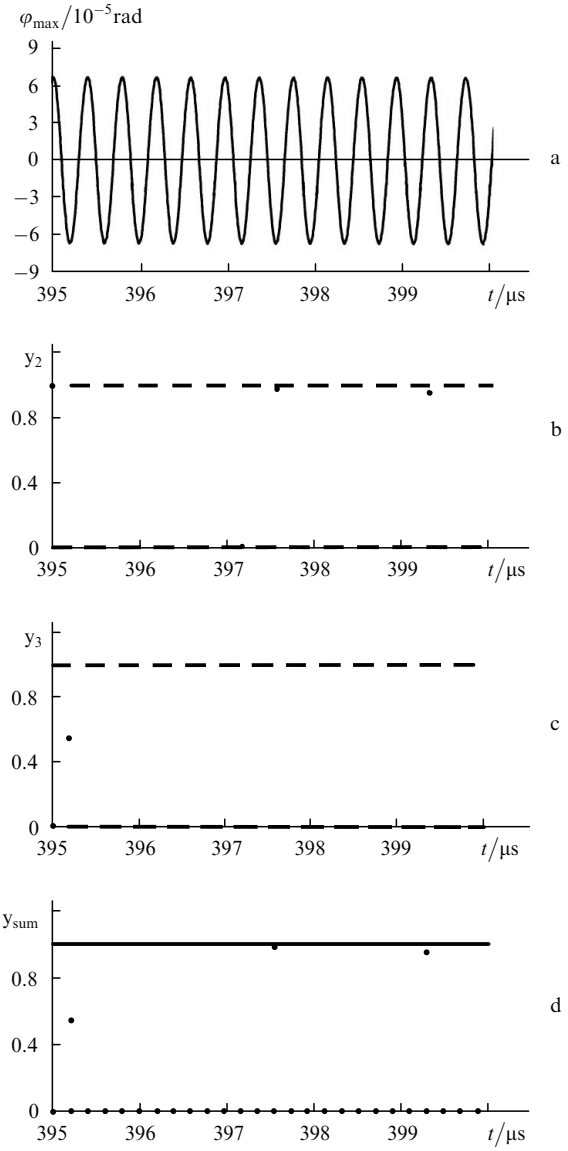

Figure 5. Angular position of the central far-field radiation maximum (a) and the NN outputs y_1, y_2, and y_{sum} (b–d).

Distributions $|F|(x/a)$ for two instants differing approximately by half the beat period and for established single-mode lasing are shown in Fig. 6a. Figures 6b–d present the dependence of the beat period, the oscillation amplitude of the angular directivity of radiation, and the oscillation amplitude of the wave intensity averaged over an aperture on the output mirror on the pump excess k over the threshold. All these parameters increase with increasing k. In the given case, the beat period for an empty resonator is 0.3884 μs, in good agreement with its values for two-model lasing (Fig. 6b). The angular far-field oscillations of the beam are consistent with those obtained in [15]. Note that the far-field oscillation amplitude of the beam revealed some nonlinearity (Fig. 6c) compared to the oscillation amplitude of the wave intensity $\bar{I}$ averaged over the aperture (Fig. 6d). As the pump power was increased, the conditions for the recognition of input distributions improved and the intermediate values of the NN outputs decreased ($y_{1-4} \sim 0.5$). The corresponding figures are similar to Figs 4b–d and 5b–d.

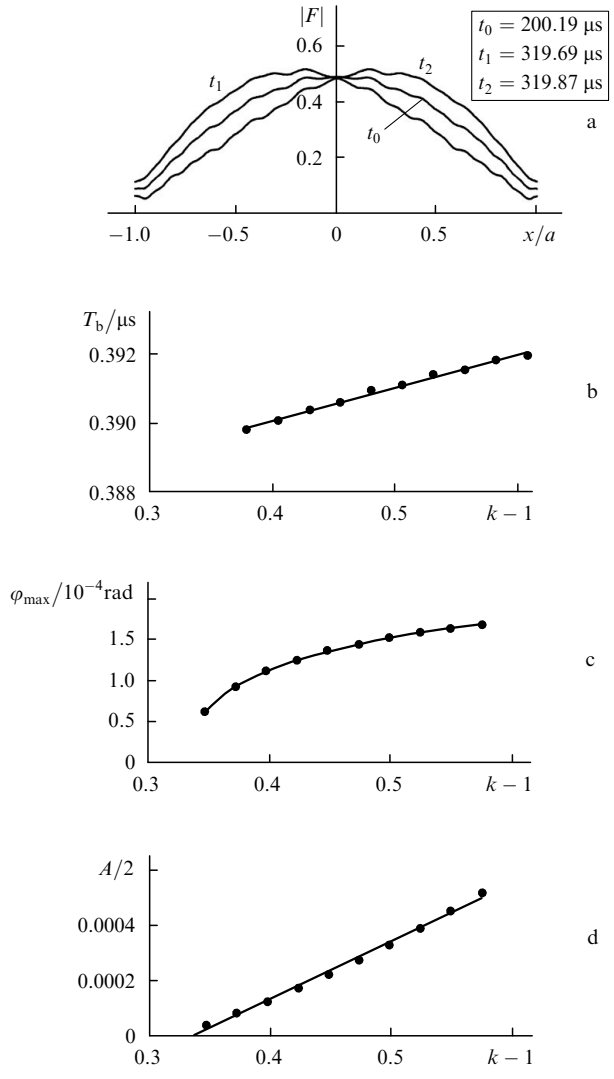

Figure 6. Regime of established beats: distributions of the modulus of the complex amplitude of radiation incident on the output mirror at the instants of maximum deviations (t_1, t_2) and upon single-mode lasing (t_0) (a), and dependences of the beat period, the oscillation amplitude of the angular directivity of radiation, and the oscillation amplitude of the average radiation intensity incident on the output mirror on the pump excess over the threshold k (b–d).

5. The slow-response neural network

The response time of pyroelectric IR detectors based on triglycinesulfate is 0.1–0.01 μs and the interval between measurements is 55.6 μs [22]. For definiteness, the response time was set equal to 0.1 μs, which is comparable with the beat period 0.39 μs. The operation of the NN with such parameters was studied for 3200 μs (Fig. 7), the output signals $y_1 - y_{sum}$ being integrated during 0.1 μs. Figure 7a shows that the NN well recognises the cessation of single-mode lasing; however, two-mode lasing is recognised by the NN with some omissions (Figs 7b, c). The omissions appear either when the counting instant falls on a comparatively symmetric distribution or a distribution with different relation between mode phases. In this case, the recognition quality can be improved by combining signals y_2 and y_3.

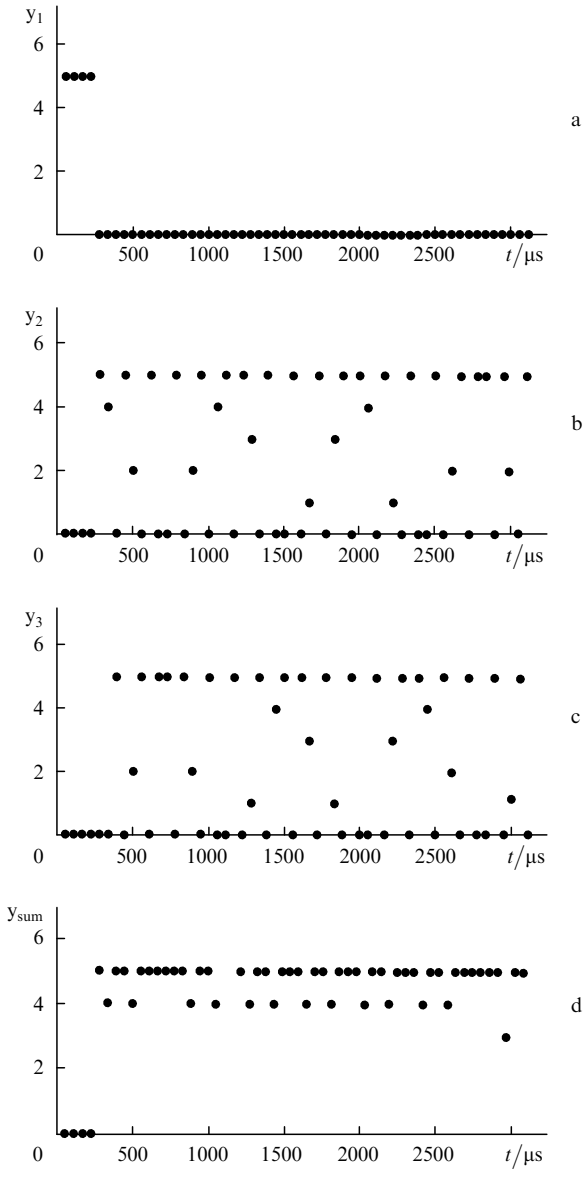

Figure 7. Simulation of the NN operation with the time response determined by a pyroelectric laser radiation detector.

The total signal is shown in Fig. 7d. One can see that omission at $y_{sum} = 5$ are compensated by smaller values of y_{sum}, which demonstrates good recognition quality.

The main advantage of the NN considered above is a small number of arithmetic operations of the processor required for obtaining the values of $y_1 - y_4$ from input signals (i.e. a small recognition time τ_{rcg}). The value of τ_{rcg} was estimated by realising the procedure of repeated recognition of input distributions without a round trip of radiation in the resonator and calculation of the gain. The number of recognition events was 320 000, and the time was measured by the system clock. For the 500-MHz Celeron processor, $\tau_{rcg} = 34.8$ μs, which is smaller than the interval between counts equal to 55.6 μs.

6. Conclusions

It has been demonstrated that a neural network can be trained by using a set of calculated distributions to recognise reliably the onset of two-mode lasing. In the author's opinion, the approach to control the mode composition proposed in the paper is acceptable in practice and makes it possible to use theoretical results more efficiently. This approach can be further developed by using improved neural networks and a better processing of their output signals to control a more complicated lasing dynamics.

Acknowledgements. The author thank N.N. Elkin for discussions of schemes for calculating transient lasing and V.N. Glebov for useful discussions of methods for detecting IR emission.

References

1. Khanin Ya.I. *Osnovy dinamiki lazerov* (Fundamentals of Laser Dynamics) (Moscow: Nauka, 1999).
2. Suchkov A.F. *Trudy FIAN*, **43**, 161 (1968).
3. Belenov E.M., Morozov V.N., Oraevsky A.N. *Trudy FIAN*, **52**, 238 (1970).
4. Staliunas K., Tarroja M.F.H., Weiss C.O. *Opt. Commun.*, **102**, 69 1993).
5. Brambilla M., Cattaneo M., Lugiato L.A., et al. *Phys. Rev. A*, **49**, 1427 (1994).
6. Prati F., Zucchetti L., Molteni G. *Phys. Rev. A*, **51**, 4093 (1995).
7. Vladimirov A.G., Skryabin D.V. *Kvantovaya Elektron.*, **24**, 913 (1997) [*Quantum Electron.*, **27**, 887 (1997)].
8. Bowers M.S., Moody S.E. *Appl. Opt.*, **29**, 3905 (1990).
9. Elkin N.N., Napartovich A.P. *Prikladnaya optika lazerov* (Applied Laser Optics) (Moscow: Atominform Central Research Institute, 1989).
10. Murphy W.D., Bernabe M.L. *Appl. Opt.*, **17**, 2358 (1978).
11. Latham W.P. Jr., Dente M.L. *Appl. Opt.*, **19**, 1618 (1980).
12. Elkin N.N. *Matem. Model.*, **2**, 104 (1990).
13. Golub G., Van Loan C. *Matrix Computations* (Baltimore: Johns Hopkins Univer. Press, 1996; Moscow: Mir, 1999).
14. Elkin N.N. *Lecture Notes in Computational Science*, **2542**, 430 (2003).
15. Elkin N.N. *Matem. Model.*, **10**, 91 (1998).
16. Elkin N.N., Napartovich A.P. *Kvantovaya Elektron.*, **30**, 1065 (2000) [*Quantum. Electron.*, **30**, 1065 (2000)].
17. Nesterov A.V., Niz'ev V.G. *Izv. Ross. Akad. Nauk, Ser. Fiz.*, **63**, 2039 (1999).
18. Huyet G., Martinoni M.C., Tredicce J.R., et al. *Phys. Rev. Lett.*, **75**, 4027 (1995).
19. Wasserman P.D. *Neural Computing: Theory and Practice* (New York: Van Nostrand Reinhold, 1989; Moscow: Mir, 1992).
20. Korneev V.V., Gareev A.F., Vasyunin S.V., et al. *Bazy dannykh, intellektual'naya obrabotka informatsii* (Data Bases and Intellectual Data Processing) (Moscow: S.V. Molgachev Izd., 2001).
21. Svelto O. *Principles of Lasers* (New York: Plenum Press, 1998; Moscow: Mir, 1990).
22. Ishanin G.G. *Priemniki izlucheniya opticheskikh i optiko-elektronnykh priborov* (Photodetectors in Optical and Optoelectronic Instruments) (Leningrad: Mashinostroenie, 1986).